Determination of the Ground-State Atomic Structures of Size-Selected Au Nanoclusters by Electron-Beam-Induced Transformation

Z. W. Wang and R. E. Palmer*

Nanoscale Physics Research Laboratory, School of Physics and Astronomy, University of Birmingham, Birmingham, B15 2TT, United Kingdom

(Received 29 January 2012; published 13 June 2012)

The equilibrium ground state atomic structures of nanoparticles are critical to understanding the relationship between their structure and functionality, e.g., in catalysis, and are the standard output of first principles and semiempirical theoretical treatments. We demonstrate a method of obtaining a stable population of the structural isomers of supported Au clusters from a metastable initial array via electron beam irradiation. Statistical investigation of size-selected Au clusters containing 923 ± 23 atoms via aberration-corrected scanning transmission electron microscopy shows that virtually all of the icosahedral (Ih) clusters undergo structural transformations into decahedral (Dh) (primarily) or fcc isomers while Dh and FCC clusters generally retain their atomic structures after electron irradiation of each cluster individually for up to 400 s at a dose of 2.4×10^4 e^-/angstrom^2/frame. Intermediate phases are often observed in the image series (videos) before the appearance of the new stable isomers, the relative structural populations of which can be controlled via the electron beam dose. The comprehensive results reported here should provide a valuable experimental reference for testing or refining potential models and for kinetic or dynamical treatments of the atomic configurations.

DOI: 10.1103/PhysRevLett.108.245502 PACS numbers: 61.46.Bc, 61.46.Df, 64.70.Nd, 68.37.Ma

Metal nanoparticles may present a range of different geometric structures (thus atomic arrangements), such as bulklike fcc arrangements and translational-symmetry-forbidden icosahedral (Ih) or decahedral (Dh) structures [1]. For size-selected atomic clusters [2–6] generated in the beam, theoretical calculations (generally at $T = 0$) far outstrip direct experimental measurements of even the as-produced configurations [7]. Thermal annealing of nanoparticles followed by electron microscopy provides valuable insights into thermally accessible structures but detailed information on the transformation process cannot be obtained since only the initial and final structures of the clusters are observed [8,9]. Fluctuations in the atomic structure of individual small metal clusters under electron beam irradiation have been well established since the 1980s [10,11]. Here we harness this effect in the aberration-corrected STEM to probe, one cluster at a time, the atomic structure of a statistical ensemble of (79) Au clusters, each containing 923 ± 23 atoms (923 is a magic number for the icosahedron, Ino-decahedron and cuboctahedron), as a function of irradiation time. We investigate the development of the population distribution as a function of time, establishing the branching ratios between different structural transformation channels (specifically, Ih to Dh or fcc) and demonstrate the intermediate atomic structures observed prior to the final, stable atomic configuration.

The size-selected Au clusters were prepared with a magnetron sputtering, gas condensation cluster beam source incorporating a lateral time-flight mass selector [12–15]. The nominal mass resolution employed was $M/\Delta M = 20$, such that the "Au_{923}" clusters contained 923 ± 23 atoms. The STEM investigation was performed with a 200 kV JEM 2100F field emission electron microscope (JEOL) with spherical aberration corrector (CEOS). Electrons scattered incoherently from the samples were recorded by a high angle annular dark field (HAADF) detector at an inner collection angle of 62 mrad and convergence angle 19 mrad. Because of the monotonic dependence of the HAADF intensity on the number of atoms in the columns [16–21], three-dimensional cluster structures can be obtained [22,23] when coupled with electron scattering simulations.

Figure 1 shows a set of HAADF images characteristic of the three main ordered structures we observe for Au_{923} clusters, i.e., Fig. 1(a), decahedron (Dh), Fig. 1(b), fcc polyhedron, and Figs. 1(c) and 1(d) icosahedron (Ih). The decahedral Au_{923} clusters, Fig. 1(a), often show a partial Marks-type surface reconstruction [11] (i.e., deviation from the Ino-Dh structure), such that reentrant structures are observed at some of the edges that separate the {100} facets while other edge(s) remain unreconstructed. Since 923 is not a magic number for the Marks decahedron, it may be that the Marks-like Au_{923} clusters grow upon smaller clusters with a symmetric Marks-Dh structure (887 is a magic number, for example), such that the reentrant sites are partially filled in. The fcc polyhedral Au_{923} clusters, Fig. 1(b), are found to exhibit various morphologies including truncated octahedron and cuboctahedron, while defects such as single twins are also present occasionally. Well-developed icosahedral Au_{923} clusters are commonly observed; Fig. 1(c) shows such a cluster

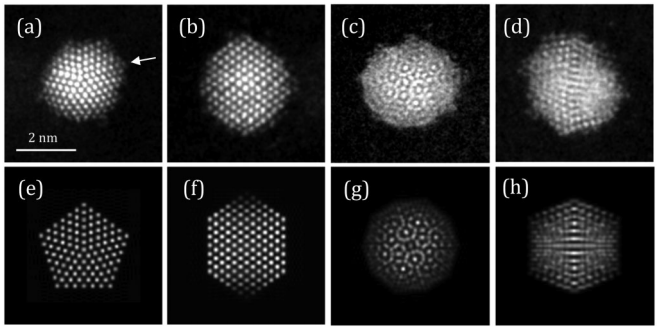

FIG. 1. Typical HAADF-STEM images of Au_{923} clusters and corresponding simulations. (a)–(d) the HAADF images for (a) a decahedron along a fivefold axis; (b) fcc polyhedron along the ⟨110⟩ axis; (c) icosahedron along a fivefold axis; and (d) icosahedron along a twofold axis, respectively. (e)–(h) the simulated images obtained from the standard atomic models of the Ino-decahedron, cuboctahedron, and icosahedron, respectively. The arrow in (a) marks the edge where no reentrant structure is observed.

orientated along a fivefold axis and Fig. 1(d) along a twofold axis. In Figs. 1(e)–1(h) we show examples of HAADF simulations, performed using the multislice method (QSTEM software package [24]) based on the standard atomic models of Ino-Dh, cuboctahedron and icosahedron, respectively, which show a good match with the experimental images of Figs. 1(a)–1(d) in terms of the atomic arrangements.

The effect of electron irradiation on the atomic structure of the Au_{923} clusters was studied systematically via the collection of a sequence of HAADF investigation for a total of 90 individual Au_{923} clusters. Each image series (movie) was recorded with a field of view of 10.5×10.5 nm, an electron dose of 2.4×10^4 e^-/angstrom^2/frame, and an acquisition time of 0.8 s/frame. We took 500 frames for all the Dh and fcc clusters and 100–500 frames for the Ih clusters [25]. In some cases a single stream of image files could not be obtained by continuous image acquisition, due to significant translational and rotational movement of the clusters during the acquisition period. In these cases, we obtained several sequences of images separated by a short interval to relocate the position of the cluster and refocus the beam. Our first investigations showed that the structural transformation process of Ih clusters could occur very fast and even arise in the process of beam alignment prior to image acquisition. To solve this problem, we first aligned the beam in one surface location and then moved the sample to a new region, rapidly taking one or several static images without beam refocusing; these images presented a large field of view but the cluster structure was still identifiable. From the static images, we selected the clusters with orientation near to a high symmetry direction ("on-axis") for movie recording.

The identification of the atomic structures of the clusters in the image series is not a trivial task since in most frames the clusters exhibit "off-axis" orientation, and beam scanning can cause their orientations to change frequently. Therefore we developed systematic STEM simulations for each of the three main atomic structures and all possible orientations of these structures, as shown in the Supplemental Material [26]; we refer to this large body of simulations as the "simulation atlas." With the help of the simulation atlas, we found that 79 out of 90 clusters studied in detail by sequential HAADF images presented identifiable atomic structures. The results of the image series for these 79 clusters are summarized in the table of Fig. 2, with a few extracts shown in the panels. The corresponding movie files for these cases can be found in the Supplemental Material [26]. The results of Fig. 2 show clearly that the icosahedron is not a stable structure because 41 out of 42 Ih clusters convert into Dh (29 out of 41) or fcc (12 out of 41) during electron beam irradiation; only 1 Ih cluster does not undergo an obvious structural transformation after 400 s of beam irradiation. By contrast, the Dh and fcc clusters appear much more stable. As indicated in Fig. 2, only 1 out of 19 fcc clusters converts to Dh, and every one of the 18 Dh clusters retains its structure during 400 s of beam irradiation. We also found that, once the structural transformations from Ih to Dh or fcc occurred, the clusters appeared rather stable; i.e., further transformations were not observed.

Systematic analysis of the movie files also allows us to measure the structural transformation times for the individual Au_{923} clusters. The precise determination of this quantity is not trivial because of similarities between the atomic arrangements of the intermediate phases observed

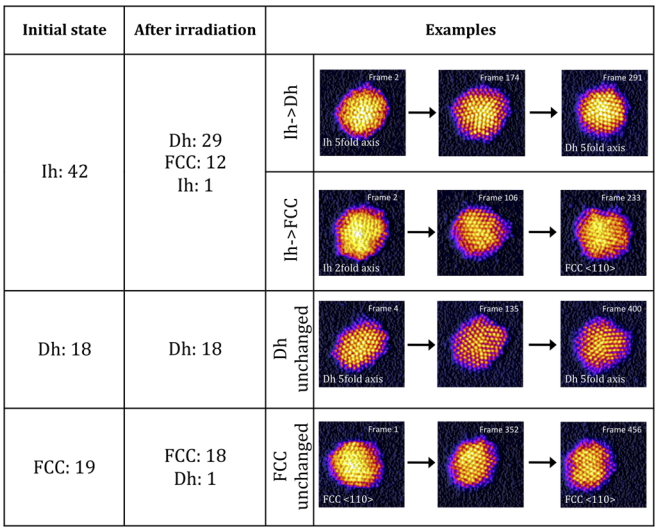

FIG. 2 (color online). Statistical results of the structural transformations obtained for 79 Au_{923} clusters. Left panel shows the structural populations of Au_{923} clusters initially and after electron beam irradiation. Right panel shows a few typical examples of structural transformation (for Ih clusters) or structural persistence (for Dh and fcc clusters).

(see below) and the newly formed stable atomic structures, especially if the cluster is in the off-axis orientation. To deal with this issue, we used 100 frames as a bandwidth and analyzed every frame in every movie file with reference to the simulation atlas to find the first band containing a new structure. The result obtained for the Ih clusters are shown in Fig. 3(a). While many Ih clusters undergo a structural transition within 80 s of electron beam irradiation, a proportion of clusters exhibit structures which do not settle until a significantly longer irradiation time (240 s). Probably this range is simply a result of the statistical nature of the transition process, but it is possible that the interaction between cluster and substrate may play a role, given that the amorphous carbon films used to support the clusters are not uniform at the atomic scale.

Based on the results of Fig. 3(a) and the corresponding data for the Dh and fcc clusters, we obtain the structural population of the 79 Au_{923} clusters studied as a function of irradiation time shown in Fig. 3(b). Here we can see a simultaneous decrease in the number of Ih clusters and increase in Dh and fcc clusters with irradiation time as a result of the structural transformations. After irradiation for 240 s no further change of the structural population is observed, indicating that the clusters have reached a stable state. Of course, the observed behavior also provides a method to control the relative population of the three ordered structures, at least to some extent, by selection of the electron beam dose.

It is worth reflecting on the nature of the stable distribution that the cluster population reaches as a result of electron beam irradiation. We can be pretty sure from the data that the icosahedral structure lies higher in energy than the decahedral and fcc structures into which it converts. Again the preference for conversion of Ih into Dh rather than fcc, by a factor of ~2.4 to 1, is consistent with the idea that Dh has the lowest energy of the three ordered structures. But we should bear in mind a cautionary note: what we are measuring is actually the "accessibility" of the final states (e.g., Dh, fcc) with respect to the initial state (e.g., Ih). It could possibly be that Dh is more accessible from Ih than is fcc because the relevant barrier(s) in the multidimensional potential energy surface is lower even though, for example, fcc may have lower energy than Dh.

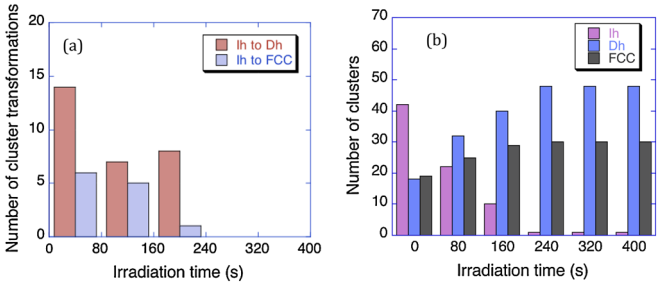

FIG. 3 (color online). Systematic investigations of the cluster structural transformation times and structural populations as a function of irradiation time. (a) Statistical distribution of transformation times from Ih to Dh or fcc. (b) The structural population of 79 Au_{923} clusters as a function of electron beam dose.

The body of data collected here should also facilitate new insights into the atomistic mechanisms of cluster structural transformations. As an illustration, analysis of the HAADF image series suggests a couple of recurring trends. (i) A range of intermediate phases often arises during the structural transitions, indicating that structural transformation is not an instantaneous process from one atomic arrangement to another. An example is shown in Fig. 4, where the initial cluster structure is Ih, as seen clearly from the image given in Fig. 4(a). After 76 s irradiation, as shown in Fig. 4(b), the cluster still resembles an icosahedron but it does not correspond to any projection of a perfect Ih cluster in the simulation atlas. Thus Fig. 4(b) is an intermediate phase arising in the transition from Ih to Dh. The same is true of Fig. 4(c), obtained after 102 s, which shows a local fivefold axis consistent with the makings of the final Dh structure, Fig. 4(d), but nucleated near the edge of the cluster. (ii) Fluctuating surface reconstructions are often observed even in image series from generally stable cluster structures, as illustrated by the occasional appearance of new surface facets; see Figs. 4(e)–4(h) for an fcc cluster.

The experimental results reported here may be compared with some previous experimental studies and theoretical calculations. As one example, a ~2 nm Au cluster prepared by *in situ* vacuum deposition on an SiO_2-covered Si substrate (smaller than size-selected Au_{923}, ~3.1 nm) showed structural transitions not only from Ih to fcc but also from fcc to Ih (i.e., the reverse transformation) during electron beam irradiation [10]. Both the cluster size and the substrate are different in this work. To explore the effect of size in our own experiments, we investigated much larger size-selected Au clusters (Au_{6000} clusters, ~5.8 nm in diameter) and recorded a series of movie files for 12

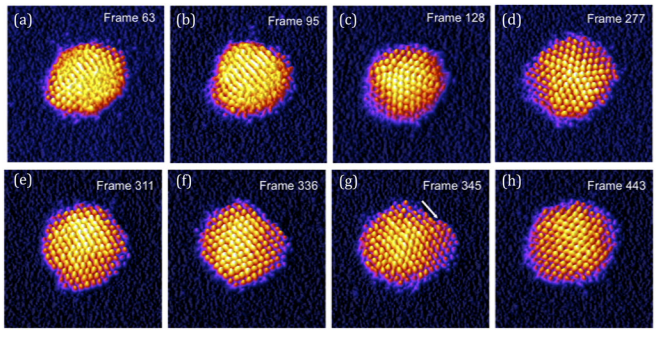

FIG. 4 (color online). Individual frames from two series of HAADF images (6 × 6 nm for each). (a)–(d) frames taken of an icosahedral cluster which undergoes a structural transition to Dh. (e)–(h) frames from a ⟨110⟩ fcc polyhedral cluster exhibiting significant surface reconstruction under electron beam irradiation. The arrow in (g) marks an incomplete surface layer nucleated as a result of surface reconstruction.

icosahedral Au_{6000} clusters with exactly the same experimental conditions as for the Au_{923} clusters. Interestingly, we found that all the Au_{6000} clusters retained their Ih structure without converting to Dh or fcc isomers, a very notable size effect. Our recent studies on very small Au clusters, such as Au_{20} and monolayer-protected Au_{38} clusters [27], exhibit continuous structural fluctuations under beam irradiation and thus provide further evidence that the beam-induced structural transformations are a function of cluster size—and smaller clusters are less stable. The effect of the substrate on cluster stability has been investigated in some previous studies [10,11]. In general, Au clusters on carbon appear more stable than Au clusters on silica under electron irradiation, presumably because the more conductive supports dissipate heating energy and charge more efficiently. A further issue to consider is the effect of the substrate on the electronic and atomic structures of the clusters [28]. In our case, low energy landing of size-selected Au clusters on amorphous carbon films retains the quasispherical shape of the clusters [29], so the interaction with the surface is rather localized.

A second point of comparison with previous work concerns the transformation from Ih to fcc which was not observed in previous thermal annealing experiments on 3–4 nm Au nanoparticles (prepared by cooling gold vapor using helium gas but without mass selection) on amorphous carbon, only the transition from Ih to Dh [8], consistent with some theoretical calculations [11,30]. It could be that the accessibility of fcc from Ih is a feature of the electron irradiation method. The possible mechanisms of electron beam interaction with the samples include not only beam heating but also momentum transfer [11,31]. In our measurements, performed at room temperature, beam heating should lead to a temperature elevation, but estimates indicate the effect should be modest considering the rather small cluster size and carbon substrate used in this work [32]. It would be intriguing to consider effects such as momentum transfer in future theoretical calculations, especially if the electron beam excitation method really does open up regions of the potential energy surface inaccessible to thermal annealing.

In summary, we have reported a substantive body of time-lapse, atomic resolution images of an ensemble of supported Au_{923} clusters viewed one at a time with the aberration-corrected scanning transmission electron microscope, demonstrating a method that drives an ensemble of 79 clusters to a stable set of structural configurations. The statistical analysis shows that electron irradiation for a maximum of 400 s at an electron dose of 2.4×10^4 $e^-/\text{angstrom}^2/\text{frame}$ causes 41 out of 42 Ih clusters to transform into Dh (29/41) or fcc (12/41) and no reverse transformations were observed. Dh and fcc clusters appear much more stable than Ih. Only one structural transformation from fcc to Dh was observed. Intermediate states are often observed in the STEM image series, providing details of the structural transformation process that we hope can be compared with dynamical theoretical models. The body of data presented also have the potential to help test and/or refine the semiempirical potentials generally used to model such nanostructures. Our experiments on an ensemble further illustrate a measure of control over the relative cluster structural populations via the electron beam dose. The general approach reported here appears to have wide application to elucidating the stable atomic structures, kinetics and atomic dynamics of clusters and other nanostructures [33–36].

We thank Ahmed Abdela for deposition of the gold clusters. We acknowledge financial support from the EPSRC and TSB. The STEM instrument employed in this research was obtained through the Birmingham Science City project "Creating and Characterising Next Generation Advanced Materials," supported by Advantage West Midlands (AWM) and in part funded by the European Regional Development Fund (ERDF).

*R.E.Palmer@bham.ac.uk

[1] M. C. Daniel and D. Astruc, Chem. Rev. **104**, 293 (2004).
[2] J. Li, X. Li, H. J. Zhai, and L. S. Wang, Science **299**, 864 (2003).
[3] B. Yoon, H. Häkkinen, U. Landman, A. S. Wörz, J.-M. Antonietti, S. Abbet, K. Judai, and U. Heiz, Science **307**, 403 (2005).
[4] O. Echt, K. Sattler, and E. Recknagel, Phys. Rev. Lett. **47**, 1121 (1981).
[5] W. D. Knight, K. Clemenger, W. A. de Heer, W. A. Saunders, M. Y. Chou, and M. L. Cohen, Phys. Rev. Lett. **52**, 2141 (1984).
[6] P. J. Roach, W. H. Woodward, A. W. Castleman, Jr., A. C. Reber, and S. N. Khanna, Science **323**, 492 (2009).
[7] F. Baletto and R. Ferrando, Rev. Mod. Phys. **77**, 371 (2005).
[8] K. Koga, T. Ikeshoji, and K. Sugawara, Phys. Rev. Lett. **92**, 115507 (2004).
[9] E. Perez-Tijerina, S. Mejia-Rosales, H. Inada and M. Jose-Yacaman, J. Phys. Chem. C **114**, 6999 (2010).
[10] S. Iijima and T. Ichihashi, Phys. Rev. Lett. **56**, 616 (1986).
[11] L. D. Marks, Rep. Prog. Phys. **57**, 603 (1994).
[12] I. M. Goldby, B. von Issendorff, L. Kuipers, and R. E. Palmer, Rev. Sci. Instrum. **68**, 3327 (1997).
[13] B. von Issendorff and R. E. Palmer, Rev. Sci. Instrum. **70**, 4497 (1999).
[14] S. Pratontep, P. Preece, C. Xirouchaki, R. E. Palmer, C. F. Sanz-Navarro, S. D. Kenny, and R. Smith, Phys. Rev. Lett. **90**, 055503 (2003).
[15] S. Pratontep, S. J. Carroll, C. Xirouchaki, C. M. Streun and R. E. Palmer, Rev. Sci. Instrum. **76**, 045103 (2005).
[16] D. D. Perovic, C. J. Rossouw, and A. Howie, Ultramicroscopy **52**, 353 (1993).
[17] D. A. Muller, Nature Mater. **8**, 263 (2009).
[18] J. M. Lebeau, S. D. Findlay, L. J. Allen, and S. Stemmer, Nano Lett. **10**, 4405 (2010).
[19] O. L. Krivanek *et al.*, Nature (London) **464**, 571 (2010).

[20] Z. W. Wang, Z. Y. Li, S. J. Park, A. Abdela, D. Tang, and R. E. Palmer, Phys. Rev. B **84**, 073408 (2011).
[21] H. Zhang, T. Watanabe, M. Okumura, M. Haruta, and N. Toshima, Nature Mater. **11**, 49 (2012).
[22] Z. Y. Li, N. P. Young, M. Di Vece, S. Palomba, R. E. Palmer, A. L. Bleloch, B. C. Curley, R. L. Johnston, J. Jiang, and J. Yuan, Nature (London) **451**, 46 (2008).
[23] S. Van Aert, K. J. Batenburg, M. D. Rossell, R. Erni, and G. Van Tendeloo, Nature (London) **470**, 374 (2011).
[24] C. Koch, Ph.D. thesis, Arizona Sate University, 2002.
[25] In some cases we took less than 500 frames for Ih clusters whose structural transformations were complete.
[26] See Supplemental Material at http://link.aps.org/supplemental/10.1103/PhysRevLett.108.245502 for simulation atlas and movies.
[27] Z. W. Wang, O. Toikkanen, B. M. Quinn, and R. E. Palmer, Small **7**, 1542 (2011).
[28] M. G. Mason, Phys. Rev. B **27**, 748 (1983).
[29] N. P. Young, Z. Y. Li, Y. Chen, S. Palomba, M. Di Vece, and R. E. Palmer, Phys. Rev. Lett. **101**, 246103 (2008).
[30] A. S. Barnard, N. P. Young, A. I. Kirkland, M. A. van Huis, and H. Xu, ACS Nano **3**, 1431 (2009).
[31] R. F. Egerton, P. Li, and M. Malac, Micron **35**, 399 (2004).
[32] V. G. Gryaznov, A. M. Kaprelov, and A. Y. Belov, Philos. Mag. Lett. **63**, 275 (1991).
[33] H. Hakkinen, Chem. Soc. Rev. **37**, 1847 (2008).
[34] M. S. Chen and D. W. Goodman, Science **306**, 252 (2004).
[35] M. Baumer and H.-J. Freund, Prog. Surf. Sci. **61**, 127 (1999).
[36] Y. Chen, R. E. Palmer, and J. P. Wilcoxon, Langmuir **22**, 2851 (2006).